

Convolutional Data Transmission System Using Real-Valued Self-Orthogonal Finite-Length Sequences

Jiong LE and Yoshihiro TANADA
Graduate School of Science and Engineering
Yamaguchi University
2-16-1 Tokiwadai, Ube, Yamaguchi, 755-8611 JAPAN

Abstract: A real-valued self-orthogonal finite-length sequence has an impulsive autocorrelation function with zero sidelobes except both shift ends. This paper presents a convolutional data transmission system using the sequence. A synchronizing sequence and a data train are convolved with another sequence, to be changed to a Gaussian signal. The signal is quantized to an integer train and transmitted through a channel, and a received signal is correlated with the respective sequences. This system suppresses a channel noise and the distortion on the amplitude limitation and the quantization and brings an impulsive synchronizing pulse to measure multipath.

Key-Words: self-orthogonal, finite-length, real-valued sequence, convolution, correlation, amplitude limitation, quantization, distortion, multipath, data transmission system.

1 Introduction

For the next generation mobile communications, the orthogonal frequency division multiplexing (OFDM) data transmission system[1] is nominated as one of the leading systems. However, the OFDM data transmission system has the defects as peak distortion, coherency slip and inter carrier interference, which must be improved by the complicated methods[2],[3].

In order to avoid such complicated methods and keep high rate transmission, we propose a convolutional data transmission system which makes the best use of the properties of a finite-length pseudonoise sequence. The sequence is a real-valued self-orthogonal finite-length sequence and its autocorrelation function has no sidelobes except left and right shift ends[4]. In this system, a data train is convolved with a sequence, to be changed to a Gaussian signal. The signal is quantized to an integer train and transmitted through a channel. The received signal is processed by a correlator. Numerical experiments show that the distortion based on amplitude limitation and quantization is suppressed through the correlation processing.

2 Real-Valued Self-Orthogonal Finite-Length Sequence

An ideal pseudonoise sequence whose autocorrelation function has no sidelobes except at both shift ends is

called a self-orthogonal finite-length sequence[4], since its shifted sequences are orthogonal in a limited shift range. In this section, the self-orthogonal finite-length sequence is explained for the application later on.

An aperiodic autocorrelation function of the self-orthogonal finite-length sequence $\{a_{M,\ell,i}\}$ of length M , member ℓ and ordinal i is expressed as

$$\begin{aligned} \rho_{M,\ell,\ell,i'} &= \frac{1}{M} \sum_{i=0}^{M-1} a_{M,\ell,i} a_{M,\ell,i-i'}^* \\ &= \begin{cases} 1 & , i' = 0 \\ \varepsilon_{M-1} & , i' = M-1 \\ \varepsilon_{M-1}^* & , i' = -(M-1) \\ 0 & , elsewhere \end{cases} \quad (1) \end{aligned}$$

where $a_{M,\ell,i} = 0$ for $i < 0$ and $i > M-1$, and i' is shift, and $*$ denotes complex conjugate. ε_{M-1} is a shift-end complex value given by

$$\varepsilon_{M-1} = |\varepsilon_{M-1}| \cdot e^{j\varphi_M} \quad (2)$$

where φ_M is phase and $j = \sqrt{-1}$. The sequence is solved by the aid of an impulse train weighted by the sequence value at every time chip T_c

$$a_{M,\ell}(t) = \sum_{i=0}^{M-1} a_{M,\ell,i} \delta(t - iT_c) \quad (3)$$

and its Fourier transform

$$A_{M,\ell}(f) = \sum_{i=0}^{M-1} a_{M,\ell,i} Z^{-i} \quad (4)$$

where $\delta(t)$ is Dirac's delta function of time t , and $Z = e^{j2\pi f T_c}$, and f is frequency. From Eq.(4), an energy spectrum of $a_{M,\ell}(t)$ is related to the autocorrelation function $\{\rho_{M,\ell,\ell,i'}\}$ of the sequence $\{a_{M,\ell,i}\}$ as

$$|A_{M,\ell}(f)|^2 = M \sum_{i'=(M-1)}^{M-1} \rho_{M,\ell,\ell,i'} Z^{-i'} \quad (5)$$

By substituting Eq.(1) to Eq.(5) and factorizing a polynomial with respect to Z^{-1} , we obtain a solution for the sequence in spectral domain[4], given by

$$A_{M,\ell}(f) = \sqrt{M|\varepsilon_{M-1}|} e^{j\varphi_M} K_{M,\ell} \times \prod_{m=0}^{M-2} \left\{ Z^{-1} - \gamma_{M,\ell,m} e^{-j\frac{\varphi_M}{M-1}} e^{j\frac{(2m+1)\pi}{M-1}} \right\} \quad (6)$$

where

$$K_{M,\ell} = 1 / \sqrt{\prod_{m=0}^{M-2} \gamma_{M,\ell,m}} \quad (7)$$

$$\gamma_{M,\ell,m} = \alpha_M \text{ or } \beta_M \quad (8)$$

$$\alpha_M = \left(\frac{1 + \sqrt{1 - 4|\varepsilon_{M-1}|^2}}{2|\varepsilon_{M-1}|} \right)^{\frac{1}{M-1}} \quad (9)$$

$$\beta_M = 1/\alpha_M \quad (10)$$

For the real-valued sequence, the phase of the shift-end correlation value is $\varphi_M = 0$ or π , and the terms with conjugate values in Eq.(6) are combined. Thus, we have four formulae according to positive or negative shift-end value of ε_{M-1} and even or odd length M .

For positive ε_{M-1} and odd M , we have the spectrum solution of the sequence $\{a_{M,\ell,i}\}$ as

$$A_{M,\ell}(f) = \sqrt{M\varepsilon_{M-1}} K_{M,\ell} \times \prod_{m=1}^{\frac{M-1}{2}} \left\{ Z^{-2} + 2\gamma_{M,\ell,m} Z^{-1} \times \cos \frac{(2m-1)\pi}{M-1} + \gamma_{M,\ell,m}^2 \right\} \quad (11)$$

by replacing m with $m + \frac{M-3}{2}$, $m = \pm 1, \pm 2, \dots$,

$\pm \frac{M-1}{2}$ in Eq.(6), where

$$K_{M,\ell} = 1 / \prod_{m=1}^{\frac{M-1}{2}} \gamma_{M,\ell,m} \quad (12)$$

For negative ε_{M-1} and odd M , we have the spectrum solution of the sequence $\{a'_{M,\ell,i}\}$ as

$$A'_{M,\ell}(f) = -\sqrt{M|\varepsilon'_{M-1}|} K'_{M,\ell} \times (Z^{-1} - \gamma'_{M,\ell,0})(Z^{-1} + \gamma'_{M,\ell,\frac{M-1}{2}}) \times \prod_{m=1}^{\frac{M-3}{2}} \left\{ Z^{-2} - 2\gamma'_{M,\ell,m} Z^{-1} \times \cos \frac{2m\pi}{M-1} + \gamma'^2_{M,\ell,m} \right\} \quad (13)$$

by replacing $m = 0, 1, 2, \dots, M-2$ with $m = 0, \pm 1, \dots, \pm \frac{M-3}{2}, \frac{M-1}{2}$ in Eq.(6), where

$$K'_{M,\ell} = 1 / \left\{ \left(\prod_{m=1}^{\frac{M-3}{2}} \gamma'_{M,\ell,m} \right) \sqrt{\gamma'_{M,\ell,0} \cdot \gamma'_{M,\ell,\frac{M-1}{2}}} \right\} \quad (14)$$

and the parameters with the mark ' are defined as similarly as those without the mark '.

We can synthesize the sequence $\{a'_{M_0,\ell,i}\}$ of length $M_0 = 2M - 1$ and shift-end negative value ε'_{M_0-1} from the sequence $\{a_{M,\ell,i}\}$ of odd length M and shift-end positive value ε_{M-1} and the sequence $\{a'_{M,\ell,i}\}$ of odd length M and shift-end negative value $\varepsilon'_{M-1} = -\varepsilon_{M-1}$. From Eqs.(11) and (13), we obtain the following spectrum of the sequence $\{a'_{M_0,\ell,i}\}$ as

$$A'_{M_0,\ell}(f) = K \cdot A_{M,\ell}(f) \cdot A'_{M,\ell}(f) \quad (15)$$

where

$$K = \frac{\sqrt{M_0|\varepsilon'_{M_0-1}|}}{M|\varepsilon_{M-1}|} \quad (16)$$

$$\alpha'_{M_0} = \alpha'_M = \alpha_M \quad (17)$$

$$\varepsilon'_{M_0-1} = -\frac{|\varepsilon_{M-1}|^2}{1 - 2|\varepsilon_{M-1}|^2} \quad (18)$$

Eq.(18) is obtained from the relation of Eq.(17).

Eq.(15) is rewritten by the standard form as

$$A'_{M_0,\ell}(f) = -\sqrt{M_0} \left| \varepsilon'_{M_0-1} \right| K'_{M_0,\ell} \times (Z^{-1} - \gamma'_{M_0,\ell,0})(Z^{-1} + \gamma'_{M_0,\ell,\frac{M_0-1}{2}}) \times \prod_{n=1}^{\frac{M_0-3}{2}} \{Z^{-2} - 2\gamma'_{M_0,\ell,n}Z^{-1} \times \cos \frac{2n\pi}{M_0-1} + \gamma'^2_{M_0,\ell,n}\} \quad (19)$$

where

$$K'_{M_0,\ell} = K_{M,\lambda} \cdot K'_{M,\lambda'} \quad (20)$$

$$\gamma'_{M_0,\ell,n} = \begin{cases} \gamma_{M,\lambda,m} & ; \quad n = 2m - 1 \\ \gamma'_{M,\lambda',m} & ; \quad n = 2m \end{cases} \quad (21)$$

Similarly, we can synthesize the sequence of odd length and shift-end negative value from the sequences of the same even lengths and shift-end positive and negative values with the same magnitude. In other words, the sequence of odd length and shift-end negative value is obtained from the convolution between a pair of sequences with the shorter same length and the shift-end positive and negative values of the same magnitude.

3 Convolutional Data Transmission by Real-Valued Self-Orthogonal Finite-Length Sequences

The pseudonoise properties of the real-valued self-orthogonal finite-length sequence are effectively utilized to a convolutional data transmission system.

Fig.1 shows signal allotment of the convolutional

data transmission system using the real-valued self-orthogonal finite-length sequences. In Fig.1(a), a synchronizing sequence $\{w a'_{M,\lambda',i}\}$ is allotted at the first half of synchronizing interval $2(M-1)T_c$ where w is the weight for the balance with data power, and a train of data $d_k \in \{+1,-1\}$, $k = 0, 1, \dots, n-1$ is allotted at the front of the data interval $N(M-1)T_c$. Convolution of the signals of Fig.1(a) with a sequence $\{a_{M,\lambda,i}\}$ makes the signals of Fig.1(b), where the signal $x_{d,i}$ and its average power P_d in the data interval are given by

$$x_{d,i} = \sum_{k=0}^{n-1} d_k a_{M,\lambda,i-k} \quad (22)$$

$$P_d = \frac{1}{N(M-1)+1} \sum_{i=0}^{N(M-1)} x_{d,i}^2 = \frac{nM}{N(M-1)+1} \quad (23)$$

and the synchronizing signal $x_{s,i}$ and its average power P_s in the synchronizing interval are given by

$$x_{s,i} = \sum_{i'=0}^{M-1} w \cdot a'_{M,\lambda',i-i'+2(M-1)} a_{M,\lambda,i'} = \frac{w}{K} a_{2M-1,\ell,i+2(M-1)} \quad (24)$$

$$P_s = \frac{w^2}{K^2} \quad (25)$$

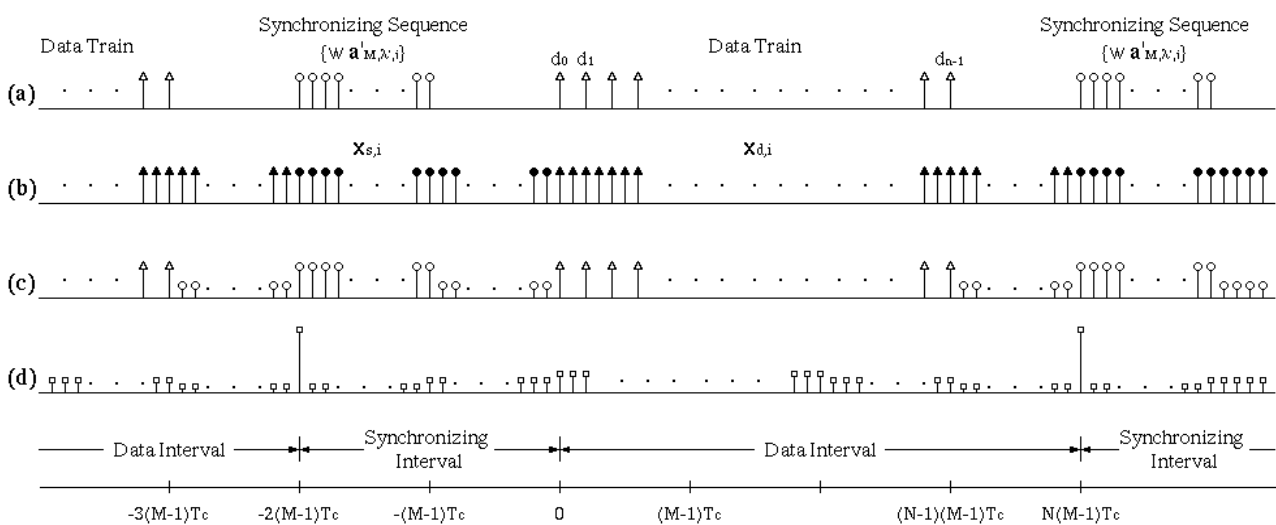


Fig.1 Signal allotment of convolutional data transmission system.

For the large number n of data, the height of the signal $x_{d,i}$ presents Gaussian distribution due to the central limit theorem. The height of the synchronizing signal $x_{s,i}$ presents approximately Gaussian distribution for the almost sequence $\{a_{2M-1,\ell,i}\}$. If we adjust these signal power to $\sigma_x^2 = P_d = P_s$, then the distribution of the height x of the signals $x_{d,i}$ and $x_{s,i}$ is approximately represented by

$$q(x) = \frac{1}{\sqrt{2\pi}\sigma_x} e^{-\frac{x^2}{2\sigma_x^2}} \quad (26)$$

In the case of $n = (N-1)(M-1) + 1$, $N \gg 1$, $M \gg 1$ and $|\varepsilon_{M-1}| \ll 1$, we obtain the followings from Eqs.(16), (18), (23) and (25)

$$\sigma_x^2 \cong M \quad (27)$$

$$K \cong \sqrt{\frac{2}{M}} \quad (28)$$

$$w \cong \sqrt{2} \quad (29)$$

The signals $x_{d,i}$ and $x_{s,i}$ of Fig.1(b) are quantized to an integer train to be transmitted. The value x_i of the signal is limited by levels $-r$ and r , and converted to the integer \hat{x}_i between $-A$ and A as follows:

$$\hat{x}_i \cong \frac{1}{K_c} x_i \quad ; \quad -r < x_i < r \quad (30)$$

$$\hat{x}_i = \begin{cases} A & ; \quad r \leq x_i \\ -A & ; \quad x_i \leq -r \end{cases} \quad (31)$$

where $r \cong K_c A$, and K_c is a coefficient so that the power of the approximated signal $K_c \hat{x}_i$ might nearly equal the power of the amplitude-limited signal in the quantization input. The height distribution of the amplitude-limited real-valued signal x'_i is given by

$$q_r(x') = q(x') \quad ; \quad -r < x < r \quad (32)$$

$$q_r(x') = \begin{cases} Q_0 \tilde{\delta}(x' - r) & ; \quad r \leq x \\ Q_0 \tilde{\delta}(x' + r) & ; \quad x \leq -r \end{cases} \quad (33)$$

where $\tilde{\delta}(x)$ is Dirac's delta function of x and

$$\begin{aligned} Q_0 &= \int_r^\infty q(x') dx' \\ &= \frac{1}{2} \operatorname{erfc}\left(\frac{r}{\sqrt{2}\sigma_x}\right) \end{aligned} \quad (34)$$

The power of the amplitude-limited signal is calculated as

$$\begin{aligned} P_r &= \int_{-\infty}^\infty x'^2 q_r(x') dx' \\ &= \sigma_x^2 \operatorname{erf}\left(\frac{r}{\sqrt{2}\sigma_x}\right) - \sqrt{\frac{2}{\pi}} r \sigma_x e^{-\frac{r^2}{2\sigma_x^2}} + 2r^2 Q_0 \\ &= r^2 - (r^2 - \sigma_x^2) \operatorname{erf}\left(\frac{r}{\sqrt{2}\sigma_x}\right) - \sqrt{\frac{2}{\pi}} r \sigma_x e^{-\frac{r^2}{2\sigma_x^2}}, \end{aligned} \quad (35)$$

and

$$\left. \begin{aligned} \sqrt{P_r} &\cong 0.718 \sigma_x \quad ; \quad r = \sigma_x \\ \sqrt{P_r} &\cong 0.960 \sigma_x \quad ; \quad r = 2\sigma_x \\ \sqrt{P_r} &\cong 0.998 \sigma_x \quad ; \quad r = 3\sigma_x \end{aligned} \right\} \quad (36)$$

The received signal \hat{x}_i is processed by a correlator with the reference sequence $\{K_c a_{M,\lambda,i}\}$, to produce the signal \tilde{x}_i shown in Fig.1(c), which is analogous to the signal in Fig.1(a). The signal \tilde{x}_i is processed by another correlator with the reference sequence $\{a'_{M,\lambda',i}\}$ to give the synchronizing pulse as shown in Fig.1(d). We can detect the data d_k in Fig.1(c) by the synchronizing pulse in Fig.1(d).

4 Numerical Experiments

We examine the proposed data transmission system by numerical experiments where $M = 65$, $N = 4$, $n = (N-1)(M-1) + 1 = 193$ and $w = \sqrt{2}$. Fig.2 shows value patterns of a pair of sequences $\{a_{65,\lambda,i}\}$ and $\{a'_{65,\lambda',i}\}$ in this experiment, where $\varepsilon_{64} = 1/65$, $\lambda = 18157114$ [5], $|a_{65,\lambda,i}|_{\max} \cong 1.9585$, $\sum_{i=0}^{64} |a_{65,\lambda,i}| \cong 49.2029$, and $\varepsilon'_{64} = -1/65$, $\lambda' = 500438969$ [5], $|a'_{65,\lambda',i}|_{\max} \cong 1.9963$, $\sum_{i=0}^{64} |a'_{65,\lambda',i}| \cong 49.6712$.

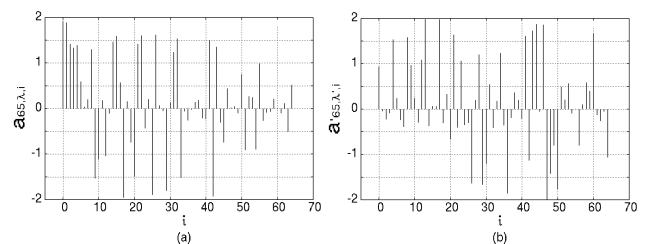


Fig.2 Patterns of a pair of sequences $\{a_{65,\lambda,i}\}$, $\{a'_{65,\lambda',i}\}$.

Fig.3 shows the signals corresponding to those of Fig.1. In Fig.3(a), the synchronizing sequence $\{a_{65,\lambda,i}\}$ is multiplied by $\sqrt{2}$, and 193 data with ± 1 values exist in the data interval $256T_c$ where T_c is omitted in the figure. In Fig.3(b), the convolved synchronizing signal $x_{s,i}$ appears rather larger in magnitude than the convolved data signal $x_{d,i}$. Fig.3(c) shows the integer signal \hat{x}_i with the limit level $r = 3\sigma_x \cong 24.2$ and the corresponding maximum integer $A = 30$ when quantized with equal division[5]. Fig.3(d) shows the correlated signal \tilde{x}_i with the reference sequence $\{a_{65,\lambda,i}\}$, that contains the small distortions based on the amplitude limitation, the quantization and the small interferences on the shift-end correlation. Fig.3(e) shows the correlated signal between \tilde{x}_i and the another reference sequence $\{a'_{65,\lambda',i}\}$, where the synchronizing pulse is obtained with peak $\sqrt{2}$ and the low sidelobes.

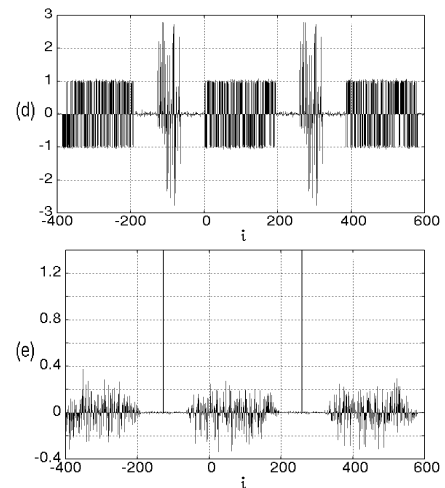
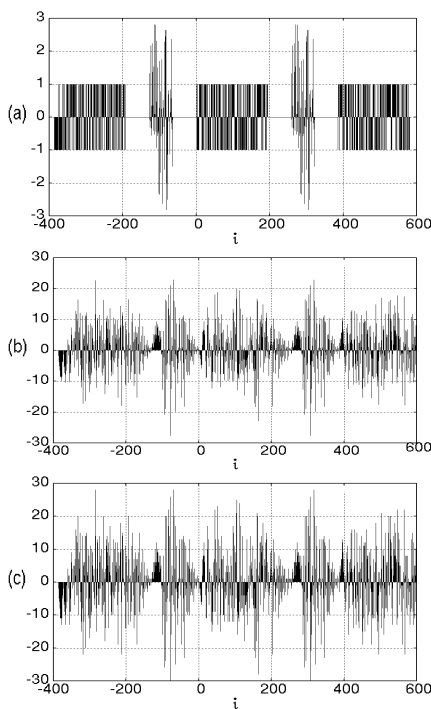


Fig.3 Signals in data transmission system. (a) Synchronizing sequence and data. (b) Convolved signal x_i . (c) Quantized signal \hat{x}_i . (d) Correlated signal \tilde{x}_i with $\{a_{65,\lambda,i}\}$. (e) Correlated signal between \tilde{x}_i and $\{a'_{65,\lambda',i}\}$.

Fig.4 shows the height distributions of the data signal $x_{d,i}$ and the synchronizing signal $x_{s,i}$. In Fig.4(a), the 2047 sets of 193 random data are loaded, and the values of the signal $x_{d,i}$ are measured at the range $64 \leq i \leq 128$ where the signal represents such statistical property as the signal of the very long data length. Fig.4(b) presents the same distribution as the value distribution of $\sqrt{65} \cdot a_{129,\ell,i}$.

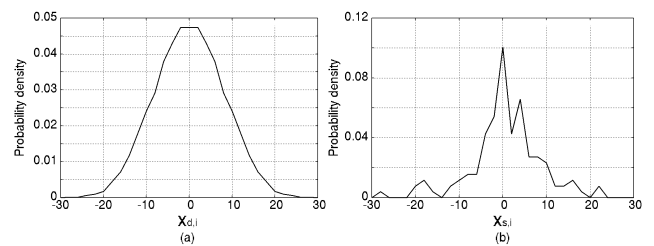


Fig.4 Height distributions of signals $x_{d,i}$ and $x_{s,i}$.

Fig.5 shows the height distributions of the correlated data signal $\tilde{x}_{d,i}$ for 100 sets of 193 random data when $A = 30$. The deviation from the mean value of data decreases as the limit level r increases, and the mean values for $r = \sigma_x \cong 8.06$, $r = 2\sigma_x \cong 16.1$ and $r = 3\sigma_x \cong 24.2$ give the values

near 0.718, 0.960 and 0.998, respectively, from Eq.(36).

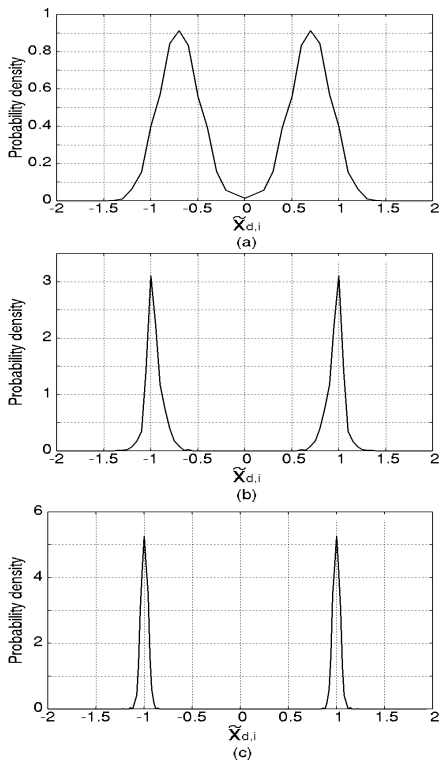


Fig.5 Height distributions of correlated data signal $\tilde{x}_{d,i}$ with $\{a_{65,\lambda,i}\}$. (a) $r = \sigma_x \cong 8.06$. (b) $r = 2\sigma_x \cong 16.1$. (c) $r = 3\sigma_x \cong 24.2$.

Fig.6 shows the distortion D of the data signal $\tilde{x}_{d,i}$ for 100 sets of 193 random data, $r = \sigma_x, 2\sigma_x, 3\sigma_x$, and A below 50, where the distortion is given by

$$D = 20 \log_{10} \frac{\sigma_d}{\mu_d} \quad (37)$$

and σ_d is the standard deviation of the distortion, and μ_d is the absolute mean value of the data.

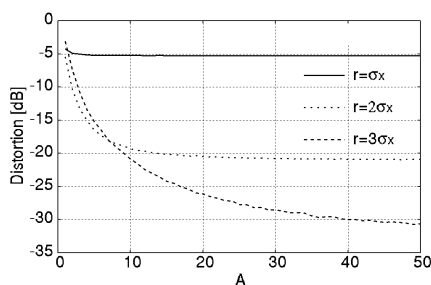


Fig.6 Output distortion.

If we decrease the rate of the loaded data, we have the smaller distortion than the distortion for the fully loaded data. From the results in Fig.6, the selection of $r = 3\sigma_x$ and A from 10 to 40 is appropriate for the practical system in the presence of additive noise.

5 Conclusion

The convolutional data transmission system using the real-valued self-orthogonal finite-length sequences is proposed. In the transmitter, the synchronizing sequence and two-valued data are convolved with the other sequence and quantized to be transmitted. In the receiver, the first correlation reconstructs the data and the second correlation gives the impulsive synchronizing pulse. This system suppresses the distortion on the amplitude limitation and the quantization as well as a channel noise and brings an impulsive synchronizing pulse to measure the multipath.

References:

- [1] R.Nee and R.Prasad, *OFDM for Wireless Multimedia Communications*, Artech House, 2000.
- [2] S.Shepherd, J.Orriss and S.Barton, Aysmtotic Limits in Peak Envelope Power Reduction by Redundant Coding in Orthogonal Frequency -Division Multiplex Modulation, *IEEE Tran. Commun.*, Vol.40, No.1, pp.5-10, January 1998.
- [3] T.M.Schmidl and D.C.Cox, Robust Frequency and Timing Synchronization for OFDM, *IEEE Tran. Commun.*, Vol.45, No.12, pp.1613-1621, December 1997.
- [4] Y.Tanada, Orthogonal Finite-Length Sequence Sets With Impulsive Autocorrelation Function, *WSEAS Tran. on Systems*, Vol.3, Issue 6, pp.2411-2416, August 2004.
- [5] J.Le and Y.Tanada, Quantizations of Real-Valued Self-Orthogonal Finite-Length Sequence and Their Effects on Correlation Performance, *Proc. of the 2nd International Workshop on Sequence Design and Its Applications in Communications*, pp.64-67, October 2005.